Geomorphology 125 (2011) 40–50

Contents lists available at ScienceDirect

Geomorphology

journal homepage: www.elsevier.com/locate/geomorph

Surface ages and rates of erosion at the Calico Archaeological Site in the Mojave Desert, Southern California

Lewis A. Owen [a,*], Teresa Davis [a], Marc W. Caffee [b], Fred Budinger [a], David Nash [a]

[a] Department of Geology, University of Cincinnati, Cincinnati, OH45521
[b] Department of Physics/PRIME Laboratory, Purdue University, West Lafayette, IN 47906, USA

ARTICLE INFO

Article history:
Received 31 March 2010
Received in revised form 10 August 2010
Accepted 25 August 2010
Available online 6 September 2010

Keywords:
Erosion
Alluvial fans
Terrestrial cosmogenic nuclides
Calico
Mojave Desert

ABSTRACT

Erosion rates and surface exposure ages were determined at the Calico Archaeological Site in the Calico Hills of the Mojave Desert, California, using ^{10}Be terrestrial cosmogenic nuclides (TCN) methods. The Calico Hills are composed of Miocene lacustrine deposits of the Barstow Formation and fanglomerates/debris flows of the Pleistocene Yermo Deposits. These deposits are highly denuded and dissected by arroyos that have surfaces armored with chert. Surface erosion rates based on cosmogenic ^{10}Be concentrations in stream sediments range from 19 to 39 m/Ma, with an average of 30.5 ± 6.2 m/Ma. Surface boulders have ^{10}Be TCN ages that range from 27 ka to 198 ka, reflecting significant erosion of the Calico Hills. The oldest boulder age (197 ± 20 ka) places a minimum limit on the age of Yermo deposits. Depth profile ages at four locations within the study area have minimum ages that range from 31 to 84 ka and erosion rate-corrected surface exposure ages ranging from 43 to 139 ka. These surface exposure ages support the view that the surfaces in Yermo deposits formed during the Late Pleistocene to latest Middle Pleistocene. This chronology has important implications for interpreting the context of possible artifacts/geofacts at the site that might provide evidence for early human occupation of North America, and for reconstructing paleoenvironment change and landscape evolution in the region.

1. Introduction

The Calico Archaeological Site in the central Mojave Desert is one of the most controversial archaeological sites in North America (Shlemon and Budinger, 1990; Fig. 1). There is equivocal evidence for the presence of humans far earlier than any other site in North America (De Lumley et al., 1988). According to its proponents, the Calico Site is a simple quarry and lithic workshop that has yielded a variety of both light-duty and heavy-duty tools and more than 60,000 technical flakes and pieces of angular debitage (flintknapping debris). The light-duty tools include a variety of scrapers (concave, notched, convex, straight-edged, end, convex side and end, strangulated, concave side and end, and thumbnail), denticulates (saw-like tools), gravers, burins (chisel-like tools), reamers, piercing tools, blades, and bladelets. Heavy-duty tools include choppers, chopping tools, hand axes, Calico Cutters (combination chopping and cutting tools), formed and unformed anvils, hammerstones, and pecking stones (Shlemon and Budinger, 1990; Budinger, 2004; Budinger et al., 2010). No homonin fossils have been found. Shlemon and Budinger (1990) reviewed controversy over the possible existence of early human at this site and stated that it can be divided into two main issues: (1) the authenticity of the artifacts, and (2) the age of the deposits and landforms in and on which they occur (Haynes, 1973; Bryan, 1978; Taylor and Payen, 1979; Meighan, 1983; Shlemon and Budinger, 1990; Meltzer, 2009). Shlemon and Budinger (1990) used geomorphic and soil-stratigraphic methods in combination with inferred association with the marine oxygen isotope stage chronology, uranium-series dating of artifact-bearing calcretes and correlations with the nearby Lake Manix beds to obtain a chronology of these alluvial fans. The results of these studies are equivocal and the age of the landforms was unresolved. In recent years, Zehfuss et al. (2001), Matmon et al. (2005), Benn et al. (2006), Frankel et al. (2007a,b) and Le et al. (2007) have used terrestrial cosmogenic nuclides (TCNs) to date alluvial fans similar to those found at the Calico site. TCN methods have the potential to date surfaces back to several hundred thousand years in the Great Basin and several million in more arid settings. We refer the reader to Gosse and Phillips (2001) who describe the principles and application of TCNs methods in great depth. Applying these techniques to the surfaces at the Calico Archaeological Site we aim to provide minimum estimates of the age of the deposits, and to quantify rates of surface erosion. We do not discuss the authenticity of the artifacts in this paper, but concentrate on defining the age of the surface and rates of surface erosion on the alluvial fans where they are found.

2. Physical setting

The Calico Arcaheological Site is ~25 km northeast of Barstow, located in the Calico Hills, east of the Calico Mountains in central

* Corresponding author. Tel.: +1 513 5564203; fax: +1 513 5566931.
E-mail address: Lewis.Owen@uc.edu (L.A. Owen).

0169-555X/$ – see front matter © 2010 Elsevier B.V. All rights reserved.
doi:10.1016/j.geomorph.2010.08.013

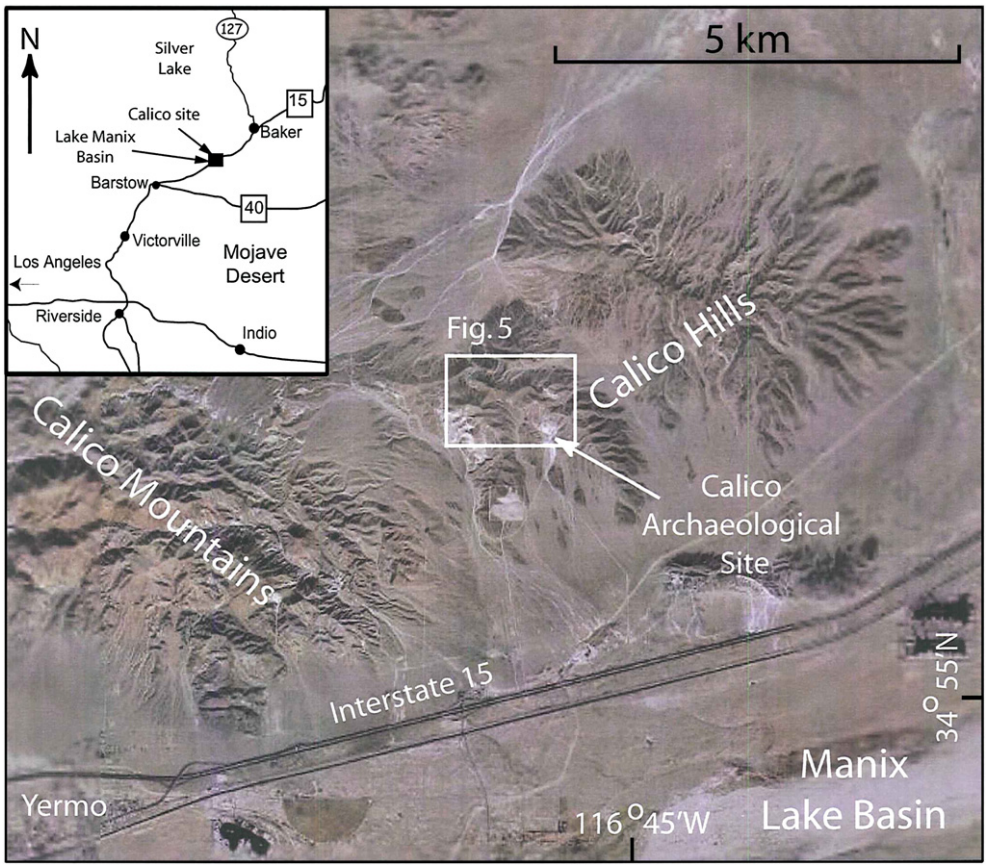

Fig. 1. Google Earth image showing the location of Calico Early Man Site in the Mojave Desert, California.

Mojave Desert. The Calico Mountains rise to 1380 m above sea level (asl) and are composed of Mesozoic volcanics, intruded and overlain by Tertiary igneous and lacustrine deposits (Fig. 2). The Calico Hills archaeological site is on a high surface at ~700 m asl that is dissected by arroyos with a maximum relative relief of 40 m (Fig. 3). The hills rise northward where they are truncated by eastward-draining steams and fans from the Calico Mountains (Fig. 3). The hills are composed of Miocene lacustrine deposits of the Barstow Formation and Pleistocene fanglomerates/debris flows of the Yermo Deposits. The Barstow Formation is mostly calcareous sedimentary rock, including mudstone, tuff, chert and mineral deposits such as bentonite. The Yermo Deposits are Pleistocene alluvial sediments; the upper section of the Yermo is composed of clasts of highly weathered tuffs and less weathered crystalline igneous rocks in a poorly sorted silty sand matrix. The unit also contains chert and limestone. The lower 1 m of the Yermo Deposits is highly calcareous,

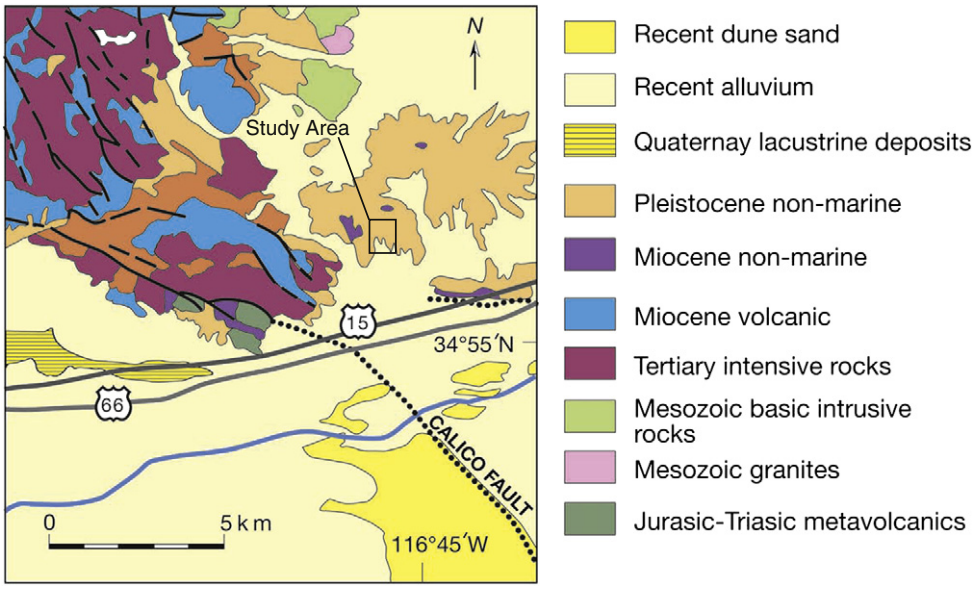

Fig. 2. Simplified geological map of the area around Calico covering approximately the same area as shown in Fig. 1 (adapted from Rogers, 1967).

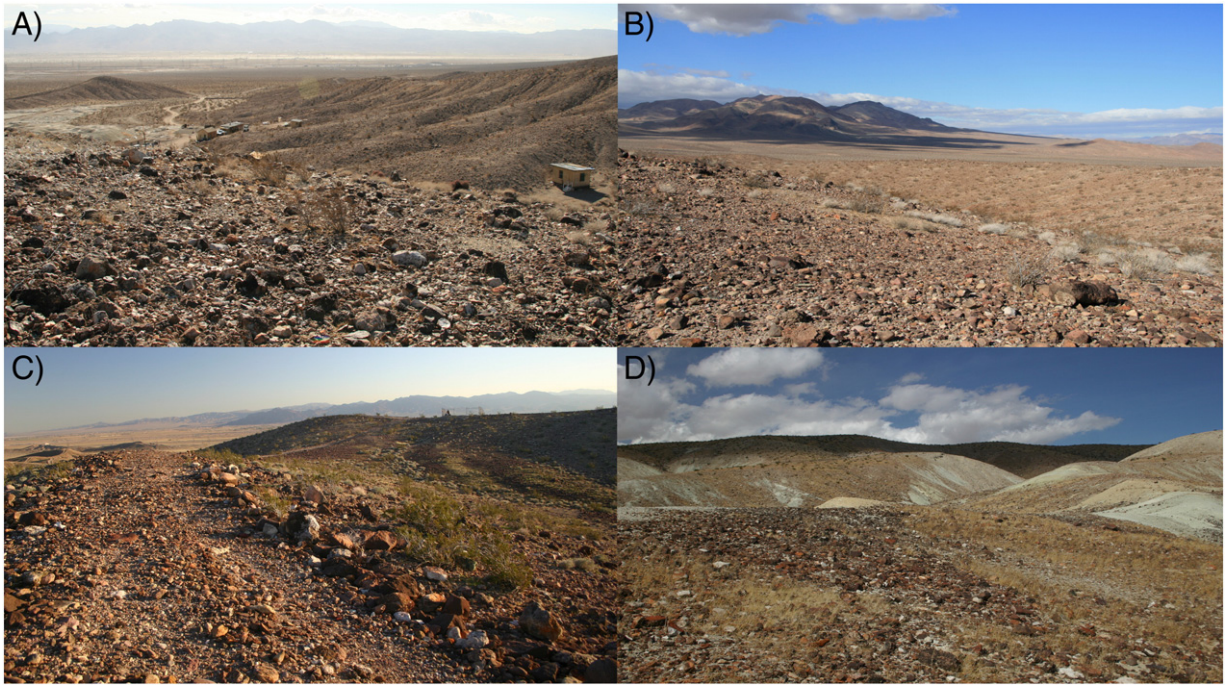

Fig. 3. Views of the geomorphology of the Calico Archaeological Site looking (A) south, (B) north and (C) east from the highest surface across the Calico archaeological site, and (D) southwest showing the eroded surfaces and exposures of the Barstow Formation.

with discontinuous calcium carbonate cementation. The stratigraphic relationships between these units are debated because there is no exposure of the contact between them. Shlemon and Budinger (1990) provide two interpretations (Fig. 4). In the first interpretation (Fig. 4A) the Yermo Deposits comprise two conformable units, the Upper and Lower Yermo Deposits, which were deposited unconformably on the Barstow Formation. The second interpretation (Fig. 4B) suggests that the Upper Yermo Deposits are a cut-fill unit in the Lower Yermo Deposits and Barstow Formation. The surfaces are armored with a residual deposit of pebble to meter-size boulders of chert. The study area is tectonically active, with several active fault systems mapped in he vicinity, including the Calico Fault and the Tin Can Alley Fault; the a latter was recently mapped by Dudash (2006). As consequence, the Bartow Formation and Yermo Deposits are slightly folded and faulted in places.

The present climate of the region is arid to semi-arid with a mean annual precipitation of ~140 mm, hot summers reaching a maximum of 46 °C and cool winters reaching a minimum of −14 °C (Shlemon and Budinger, 1990; Hereford et al., 2007). The climate is influenced by large-scale changes in Pacific Ocean sea-surface temperature caused by ENSO and Pacific Decadal Oscillation forcing (Cayan et al., 1998, 1999); wet winters tend to correspond with El Niño events.

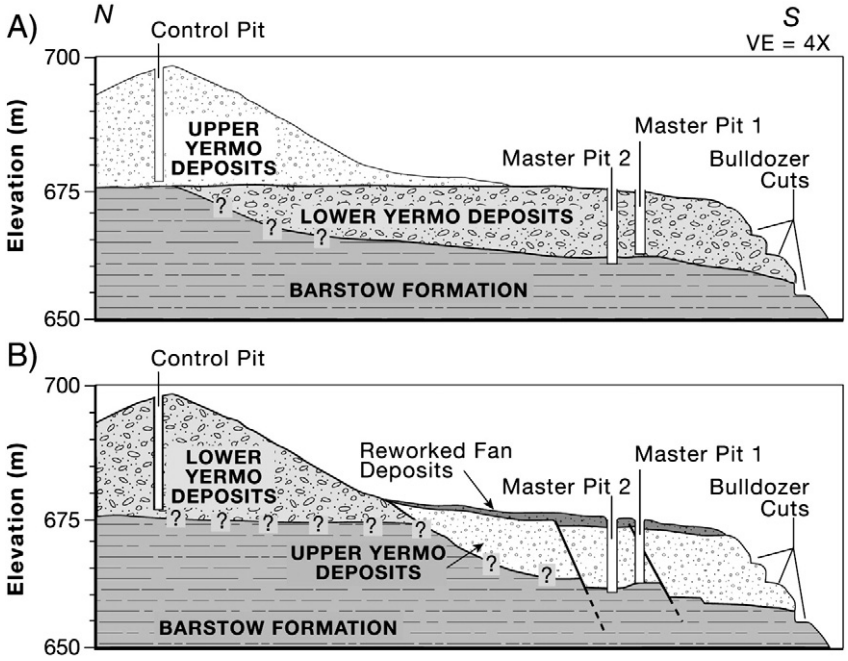

Fig. 4. Schematic sections that show the alternative hypotheses for the stratigraphy at the Calico Archaeological Site (after Shlemon and Budinger, 1990). (A) Master pits penetrating inferred artifact-bearing beds in the lower (older) Yermo Deposits; and (B) artifact-bearing (younger) beds inset into lower, tectonically tilted possibly Yermo beds.

Major cool-season storms are produced by extratropical cyclones of the north Pacific that are associated with synoptic tropospheric depressions driving a southward expansion of the Aleutian low-pressure center. The cool-season storms produce widespread, long-duration, low-intensity precipitation. The warm-season storms are convective and provide brief, local, and commonly intense rainfall. Infrequently occurring tropical cyclones and hurricanes form in the tropical Pacific Ocean occasionally during the fall. Vegetation is sparse and is dominated by xerophytic brushes, notably creosote scrub bushes.

The Quaternary history of the region has attracted much attention; recent studies are summarized in Enzel et al. (2003). During glacial times the region was cooler and wetter (Van Devender, 1990), and extensive lakes were present throughout the Mojave (Enzel et al., 2003), including Lake Manix to the immediate south of the Calico Archeaological Site. Lake Manix was feed by the Mojave River and overflowed via the Afton Canyon into Lake Mojave, present-day Soda Lake (Meek, 1989, 1990, 1999; Cox et al., 2003).

3. Methods

The study area, which includes the catchment area of the upland region that enclosed the Calico Archaeological Site, is shown in Fig. 2.

3.1. Mapping

A topographic map was constructed using a Thales ProMark 3 differential GPS with a horizontal and vertical accuracy of ±2 cm and ±5 cm, respectively. The data points were plotted using ArcMap to produce a topographic map with contour intervals of 2 m (Fig. 5).

3.2. Sampling

Samples for TCN analysis were collected from surface boulders, four pits and contemporary sediment deposits (Figs. 6–9). Boulders samples were obtained from the top few centimeters of unweathered horizontal surfaces at three different locations; the highest surface, a lower surface and an immediate elevation (Fig. 7). Four pits were dug to ~2 m depth and sediment samples were collected at 5-cm intervals down the profile (Fig. 8). At least 1 kg of sediment was collected from the surface of active channels to determine TCN concentrations for erosion rate analysis (Fig. 9). The latitude, longitude, elevation, and aspect were recorded for each of the samples (Table 1; Fig. 6).

3.3. TCN analysis

All the samples were prepared in the geochronology laboratories at the University of Cincinnati. The channel sediment samples were

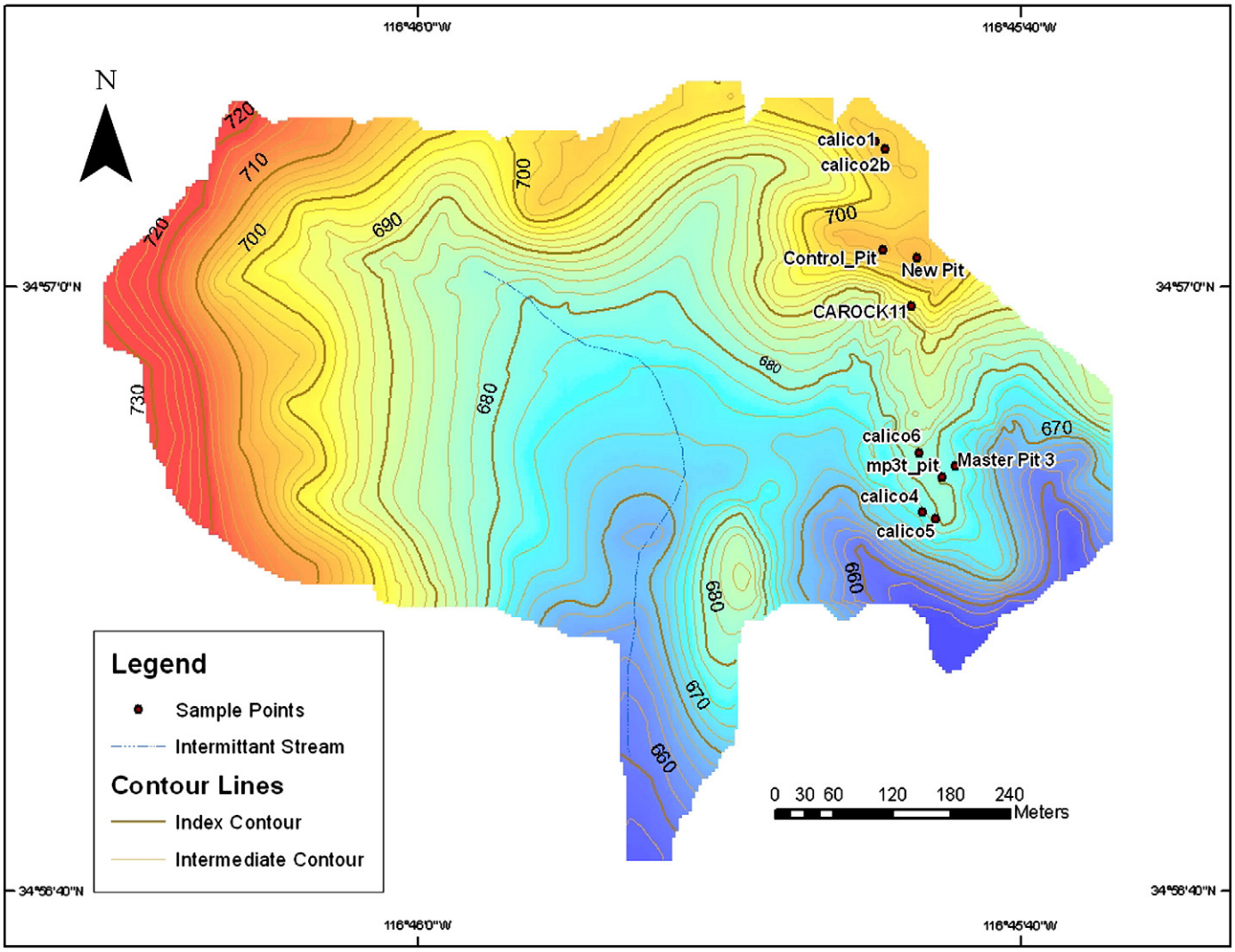

Fig. 5. Topographic map of the study area based on differential GPS surveying.

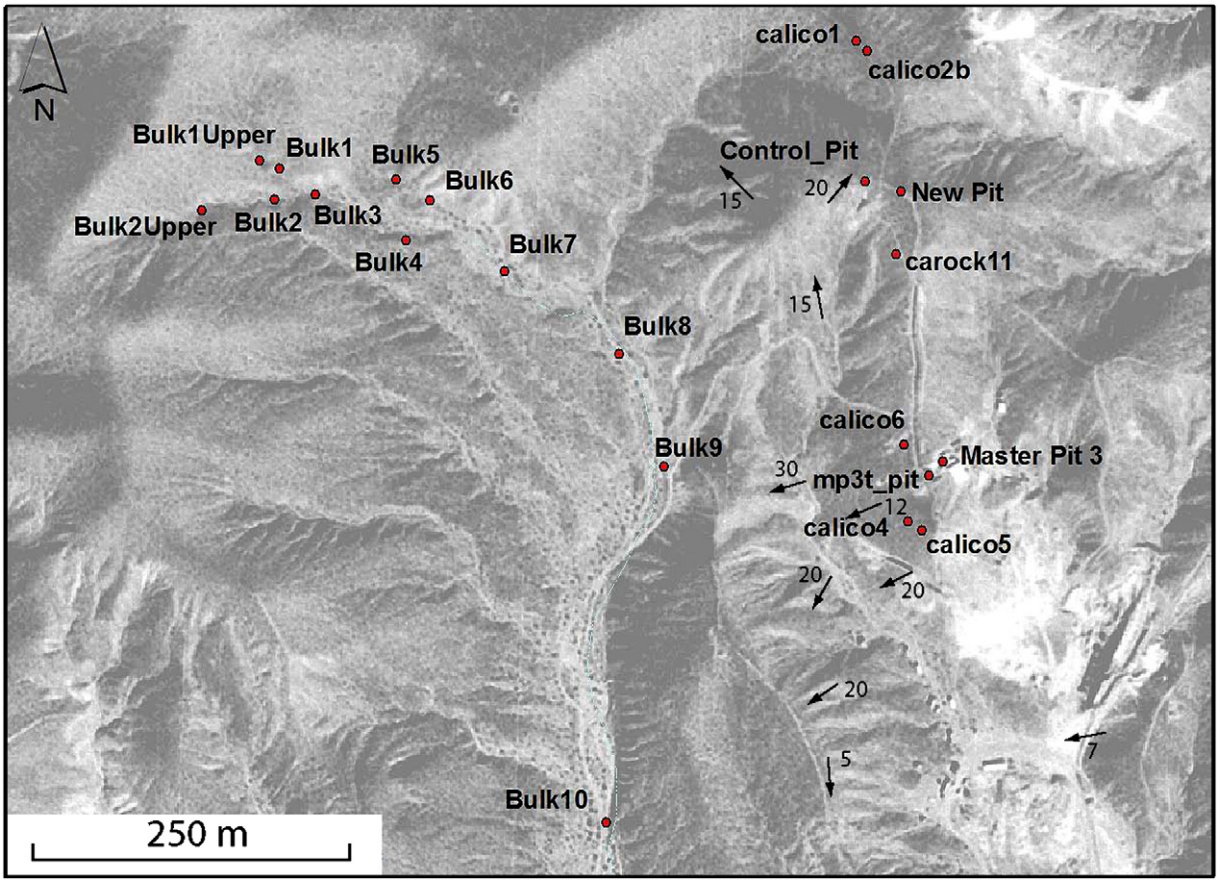

Fig. 6. Orthophoto of the Calico Hills showing the locations of the sampling sites for ^{10}Be TCNs. See Table 1 for the descriptions of the samples. The black arrows show the dip of the beds in the Yermo Formations around the pits for the depth profiles.

oven dried and sieved to obtain the 250–500 μm size fraction. One sediment sample (Bulk 3(crushed) CA028) was also crushed using the 500–2000 μm size fraction and sieved to obtain the 250–500 μm size fraction to test the possible influence of grain size on TCN concentrations. Sediment samples from the depth profiles were crushed and sieved and the 250–500 μm fraction was collected. Surface boulder samples were also crushed and the 250–500 μm size fraction was collected for processing.

The 250 to 500 μm size fraction from each sample was chemically leached by a minimum of four acid treatments: aqua regia for >9 h; two 5% HF/HNO_3 leaches for ~24 h; and one or more 1% HF/HNO_3 leaches each for ~24 h. To remove acid-resistant and mafic minerals, heavy liquid (density of 2.7 g/cm^3) separations with lithium heteropolytungstate (LST) were used after the first 5% HF/HNO_3 leach. Low background ^{9}Be carrier (six ^{10}Be/^{9}Be blanks were used with an average value of $3.2 \pm 0.7 \times 10^{-15}$) was added to pure quartz and dissolved in concentrated HF and then fumed with perchloric acid. Chemical blanks were processed using the reagents required for a 15 g quartz sample. Next, the samples were passed through anion and cation exchange columns to separate the ^{10}Be fraction. Ammonium hydroxide was added to the ^{10}Be fractions to precipitate beryllium hydroxide gel. The beryllium hydroxide was oxidized by ignition at 750 °C for 5 min in quartz crucibles. Beryllium oxide was mixed with Nb powder and loaded in steel targets for the measurement of the

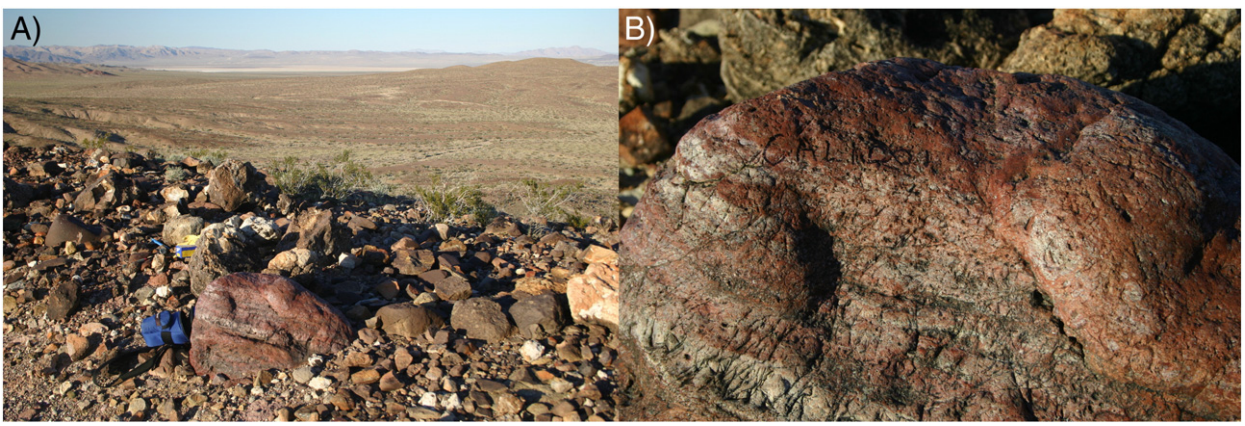

Fig. 7. Typical setting (A) and nature (B) of the surface boulders (calico1) that were sampled for ^{10}Be TCN surface exposure dating at the Calico Archaeological Site.

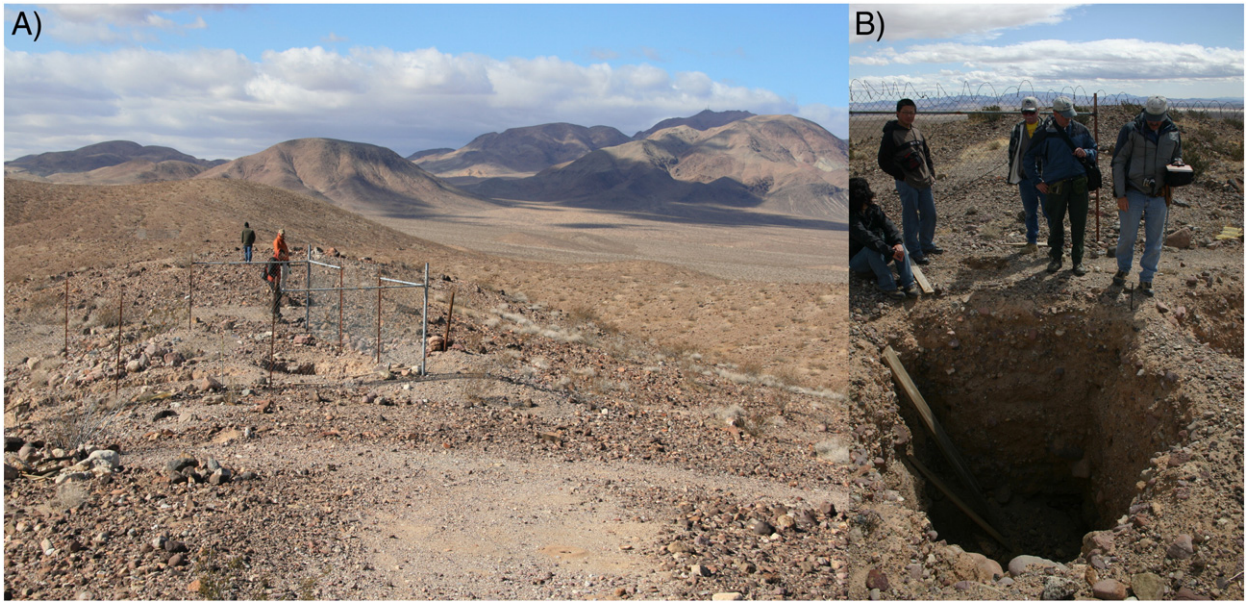

Fig. 8. View of a typical pit (Control Pit) that was used to collect depth profile samples for terrestrial cosmogenic nuclide analysis. (A) View looking west at pit and (B) view into pit showing fanglomerates.

$^{10}Be/^{9}Be$ ratios by accelerator mass spectrometry at the PRIME Laboratory at Purdue University.

All ^{10}Be TCN ages for boulders samples were calculated using the CRONUS Age Calculator 2.2 (Balco et al., 2008). This uses the scaling factors of Stone (2000) and a sea-level low-latitude production rate of 4.5 ± 0.3 ^{10}Be atoms/gram of quartz/year and a ^{10}Be half life of 1.36×10^{6} years. Isotope ratios were normalized to ^{10}Be standards prepared by Nishiizumi et al. (2007). No correction was made for geomagnetic field variations due to the ongoing debate regarding which correction factors are most appropriate (Balco et al., 2008). Geomagnetic corrections on our TCN ages can vary by up to 20%. Furthermore, we have not made any corrections for erosion for surface boulders. As a guide, assuming that all the boulders eroded at 5 m/Ma (Small et al., 1997; summit boulder erosion rate), a calculated

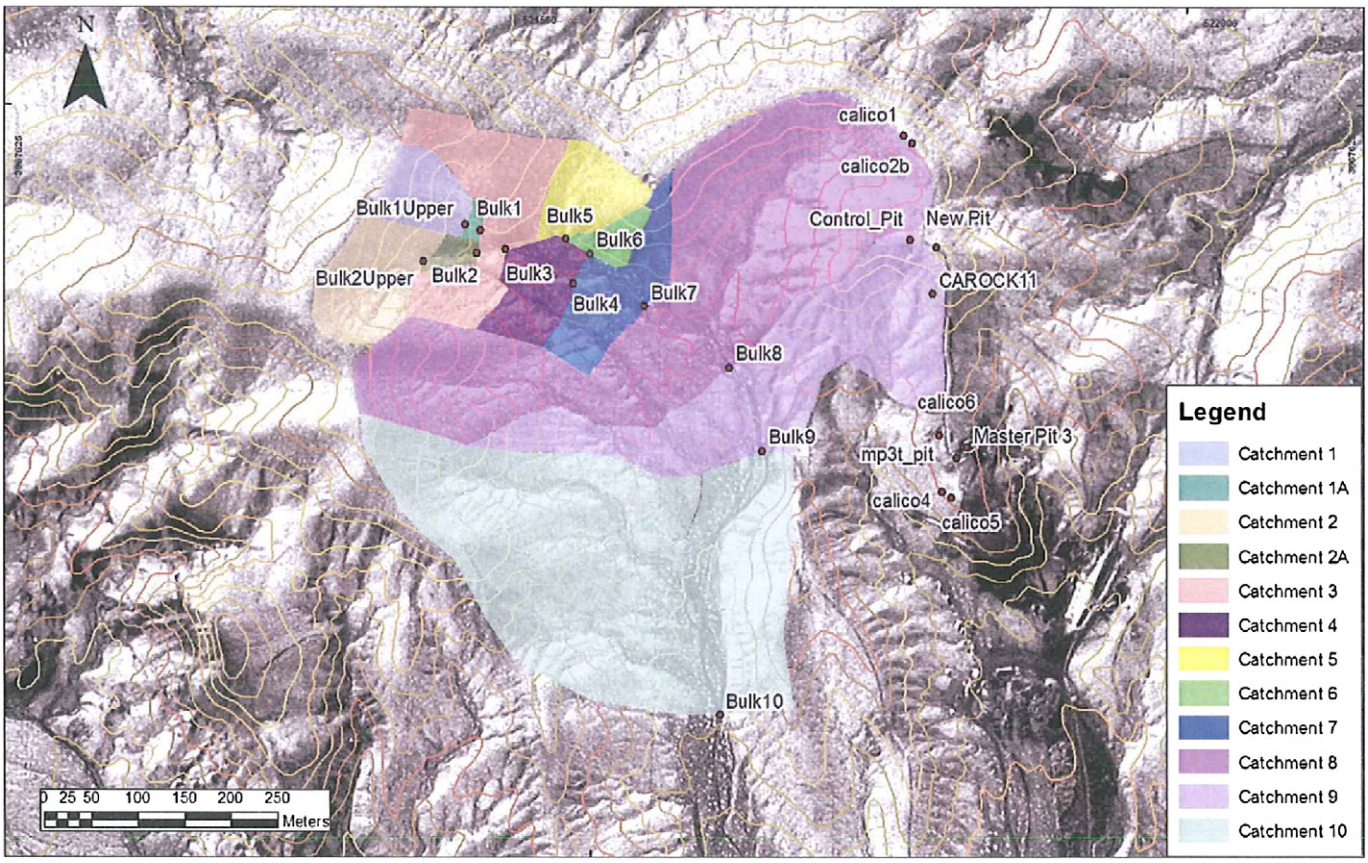

Fig. 9. Location and source areas (labeled watersheds) for sediment that was collected to determine erosion rates using the concentrations of ^{10}Be TCNs.

Table 1
Sampling locations, TCN data, ages and erosion rates.

Sample ID	Laboratory number	Latitude (°N)	Longitude (°W)	Altitude (m asl)	Depth (m)	Boulder height/width (m)	^{10}Be (10^6 atoms/g)	Age (ka)	^{10}Be erosion rate (m/Ma)
Boulders									
calico1	calico1	34.9513	116.7625	704.7	0.00	0.35/0.70	0.710 ± 0.040	92.4 ± 9.8	7.7 ± 0.8
calico2b	calico2b	34.9513	116.7624	704.8	0.00	0.12/0.90	0.409 ± 0.018	52.7 ± 5.2	14.1 ± 1.2
calico4	calico4	34.9479	116.7620	675.8	0.00	0.18/0.40	1.100 ± 0.036	148.4 ± 14.3	4.6 ± 0.4
calico5	calico5	34.9479	116.7619	676.8	0.00	0.18/0.60	0.644 ± 0.037	84.9 ± 9.1	8.5 ± 0.8
calico6	calico6	34.9485	116.7620	678.6	0.00	0.42/0.70	1.450 ± 0.068	197.7 ± 20.5	3.3 ± 0.3
CAROCK11	CA018	34.9498	116.7621	695.0	0.00	0.45/1.00	0.206 ± 0.005	26.6 ± 2.4	29.5 ± 2.2
Depth profiles									
Master Pit 3									
MP325cm	CA001	34.9483	116.7617	675.9	0.25	n/a	0.124 ± 0.005	See Fig. 12	n/a
MP350cm	CA002	34.9483	116.7617	675.9	0.50	n/a	0.109 ± 0.004	See Fig. 12	n/a
MP375cm	CA003	34.9483	116.7617	675.9	0.75	n/a	0.086 ± 0.003	See Fig. 12	n/a
MP3100cm	CA004	34.9483	116.7617	675.9	1.00	n/a	0.072 ± 0.002	See Fig. 12	n/a
MP3125cm	CA005	34.9483	116.7617	675.9	1.25	n/a	0.061 ± 0.005	See Fig. 12	n/a
MP3150cm	CA006	34.9483	116.7617	675.9	1.50	n/a	0.050 ± 0.003	See Fig. 12	n/a
MP3175cm	CA007	34.9483	116.7617	675.9	1.75	n/a	0.081 ± 0.020	See Fig. 12	n/a
MP3195cm	CA008	34.9483	116.7617	675.9	1.95	n/a	0.037 ± 0.002	See Fig. 12	n/a
New Pit									
NP25cm	CA013	34.9503	116.7621	705.1	0.25	n/a	0.237 ± 0.007	See Fig. 12	n/a
NP50cm	CA014	34.9503	116.7621	705.1	0.50	n/a	0.182 ± 0.006	See Fig. 12	n/a
NP75cm	CA015	34.9503	116.7621	705.1	0.75	n/a	0.167 ± 0.006	See Fig. 12	n/a
NP100cm	CA016	34.9503	116.7621	705.1	1.00	n/a	0.126 ± 0.005	See Fig. 12	n/a
NP125cm	CA009	34.9503	116.7621	705.1	1.25	n/a	0.102 ± 0.005	See Fig. 12	n/a
NP150cm	CA010	34.9503	116.7621	705.1	1.50	n/a	0.091 ± 0.003	See Fig. 12	n/a
NP175cm	CA011	34.9503	116.7621	705.1	1.75	n/a	0.084 ± 0.004	See Fig. 12	n/a
NP200cm	CA012	34.9503	116.7621	705.1	2.00	n/a	0.080 ± 0.004	See Fig. 12	n/a
MP3T Pit									
mp3t25	mp3t25	34.9482	116.7618	678.0	0.25	n/a	0.208 ± 0.013	See Fig. 12	n/a
mpt3t75	mpt3t75	34.9482	116.7618	678.0	0.75	n/a	0.130 ± 0.006	See Fig. 12	n/a
mpt3t125	mpt3t125	34.9482	116.7618	678.0	1.25	n/a	0.083 ± 0.007	See Fig. 12	n/a
mpt3t175	mpt3t175	34.9482	116.7618	678.0	1.75	n/a	0.048 ± 0.007	See Fig. 12	n/a
mpt3t225	mpt3t225	34.9482	116.7618	678.0	2.25	n/a	0.035 ± 0.006	See Fig. 12	n/a
Control Pit									
TPCP1_50	TPCP1_50	34.9503	116.7624	703.8	0.50	n/a	0.255 ± 0.016	See Fig. 12	n/a
TPCP1_100	TPCP1_100	34.9503	116.7624	703.8	1.00	n/a	0.156 ± 0.010	See Fig. 12	n/a
TPCP1_150	TPCP1_150	34.9503	116.7624	703.8	1.50	n/a	0.139 ± 0.021	See Fig. 12	n/a
TPCP1_200	TPCP1_200	34.9503	116.7624	703.8	2.00	n/a	0.114 ± 0.006	See Fig. 12	n/a
TPCP1_250	TPCP1_250	34.9503	116.7624	703.8	2.50	n/a	0.105 ± 0.012	See Fig. 12	n/a
Stream sediments									
Bulk1Upper	CA023	34.9505	116.7676	696.3	0-0.02	n/a	0.286 ± 0.028	n/a	20.8 ± 2.6
Bulk1	CA024	34.9504	116.7674	694.4	0-0.02	n/a	0.183 ± 0.008	n/a	33.5 ± 2.8
Bulk2Upper	CA025	34.9501	116.7681	699.0	0-0.02	n/a	0.168 ± 0.008	n/a	36.8 ± 3.1
Bulk2	CA026	34.9502	116.7675	694.1	0-0.02	n/a	0.196 ± 0.009	n/a	31.1 ± 2.7
Bulk3 (sieved)	CA027	34.9503	116.7671	690.0	0-0.02	n/a	0.173 ± 0.009	n/a	35.4 ± 3.1
Bulk3(crushed)	CA028	34.9503	116.7671	690.0	0-0.02	n/a	0.173 ± 0.005	n/a	35.3 ± 2.7
Bulk4	CA030	34.9499	116.7663	684.3	0-0.02	n/a	0.201 ± 0.007	n/a	30.1 ± 2.4
Bulk5	CA031	34.9504	116.7664	686.0	0-0.02	n/a	0.313 ± 0.014	n/a	18.7 ± 1.6
Bulk6	CA032	34.9502	116.7661	682.9	0-0.02	n/a	0.258 ± 0.008	n/a	22.9 ± 1.8
Bulk7	CA033	34.9497	116.7655	680.6	0-0.02	n/a	0.188 ± 0.008	n/a	32.2 ± 2.7
Bulk8	CA034	34.9491	116.7645	676.1	0-0.02	n/a	0.197 ± 0.008	n/a	30.6 ± 2.5
Bulk9	CA035	34.9483	116.7641	673.4	0-0.02	n/a	0.158 ± 0.006	n/a	38.5 ± 3.1
Bulk10	CA036	34.9458	116.7646	662.0	0-0.02	n/a	0.192 ± 0.014	n/a	31.1 ± 3.2

age of 10 ka assuming zero boulder erosion would underestimate the true age by a maximum of 4%; an age of 20 ka by 9%; an age of 40 ka by 20% (c.f. Owen et al., 2002).

Basin-wide erosion rates were calculated using the ^{10}Be concentrations of the stream sediment applying the methods of Bierman and Steig (1996) and Lal's (1991) equation for an eroding Earth surface, where:

$$\varepsilon = \frac{\Lambda}{\rho}\left(\frac{P(0)}{N_i} - \lambda\right) \quad (1)$$

Where, N_i is inherited activity (atoms ^{10}Be/g quartz), $P(0)$ is the production rate at the surface, ε is erosion rate (cm/year), ρ is density of the target material (g/cm^3), and Λ is attenuation length (160 g/cm^2). Catchment-wide TCN production rates were calculated using the median altitude since the relative relief was small (<50 m). To test for bias of erosion rates due to heterogeneous sediment mixing and/or influence of catchment size two large catchment areas were examined, each with small sub-basins. The area of catchment above each sample was derived from GIS analysis of the topographic map (Fig. 9) that was stored in the GIS. The size of the catchment increased progressively down drainage so that the catchment for each progressively lower sample was the sum of each catchment above the sample (Table 2).

If a geomorphic surface has not been eroded then the concentration of TCN will decrease exponentially with depth below the surface. The rate at which nuclide production decreases is a function of the density of the material through which the cosmic rays are passing. In general, production rates decrease by 1/*e* for every ~160 g/cm^2 for increasing depth. This absorption length is equivalent to ~80 cm in alluvial fans. Therefore, by ~2.4 m depth, production of TCNs is negligible (Anderson et al., 1996; Hancock et al., 1999; Gosse and

Table 2
Details of catchment areas.

Catchment name	Area of catchment (m^2)	Area of catchment (km^2)	Sample number	Area of catchment for sample	Area of catchment (km^2)	Maximum altitude of catchment (m asl)	Minimum altitude of catchment (m asl)	Median altitude of catchment (m asl)	Altitude of sample location (m asl)
1	7169	0.0072	Bulk1upper	Catchment 1	0.0072	725.4	696.3	710.4	696.3
1A	622	0.0006	Bulk1	Catchments 1 + 1A	0.0078	725.4	694.4	709.4	694.4
2	12355	0.0124	Bulk2upper	Catchment 2	0.0124	726.9	699.0	712.5	699.0
2A	1569	0.0016	Bulk2	Catchments 2 + 2A	0.0139	726.9	694.1	710.1	694.1
3	19830	0.0198	Bulk3	Catchments 1 + 1A + 2 + 2A + 3	0.0415	725.4	690.0	707.2	690.0
4	6479	0.0065	Bulk4	Catchments 1 + 1A + 2 + 2A + 3 + 4 + 5 + 6	0.0587	726.9	684.3	705.1	684.3
5	8032	0.0080	Bulk5	Catchment 5	0.0080	726.9	686.0	706.0	686.0
6	2657	0.0027	Bulk6	Catchments 5 + 6	0.0107	726.9	682.9	704.4	682.9
7	11491	0.0115	Bulk7	Catchments 1 + 1A + 2 + 2A + 3 + 4 + 5 + 6 + 7	0.0702	726.9	680.6	703.3	680.6
8	88050	0.0881	Bulk8	Catchments 1 + 1A + 2 + 2A + 3 + 4 + 5 + 6 + 7 + 8	0.1583	726.9	676.1	701.0	676.1
9	44972	0.0450	Bulk9	Catchments 1 + 1A + 2 + 2A + 3 + 4 + 5 + 6 + 7 + 8 + 9	0.2032	726.9	673.4	699.7	673.4
10	96454	0.0965	Bulk10	Catchments 1 + 1A + 2 + 2A + 3 + 4 + 5 + 6 + 7 + 8 + 9 + 10	0.2997	726.9	662.0	694.0	662.0

Phillips, 2001). The TCN concentration of samples collected from a depth profile (usually samples collected in 10–20 cm increments from the surface to ~2 m below the surface) should decrease exponentially with depth. An exponential curve through the TCN concentrations of samples versus depth can then be extrapolated upwards to the surface, thereby constraining the age of the surface (Anderson et al., 1996; Hancock et al., 1999). However, if there had been significant erosion of the surface, then the depth profile age represents a minimum value, presuming there had been no prior exposure of the sediment to cosmic rays. Depth profiles can also be used to check for prior exposure of the sediment to cosmic rays, which results in inherited TCNs, by examining the shape of the depth curve for TCN concentrations (e.g., Anderson et al., 1996; Hancock et al., 1999). The depth profile itself cannot provide both a surface age and an erosion rate. However, if an independent estimate of erosion can be obtained, for example, from stream sediments, a model surface age can be determined from the extrapolated depth profile TCN concentrations. Finally, the shape of the concentration profile indicates whether the upper several meters, i.e. the depth sampled, has been stable over the period of exposure to cosmic rays.

Table 1 lists the TCN concentrations of the depth profiles. Sediment densities measured in top 25 cm in the field were 1.9 ± 0.1 g/cm^3. For each of the depth profiles we fitted a trend through the data using an attenuation length of 160 g/cm^2 and a density of 1.9 g/cm^3. Three ages for each surface were calculated using a weighted least squared minimization technique. In the first, we assume no erosion and no inheritance. The best-fit age was obtained by minimizing the weighted squares of the difference between the measured ^{10}Be concentrations and the concentration for a given age. We iteratively obtained the age that minimizes the sum of the squares for all samples in a profile. For the best-fit ages assuming inheritance we simultaneously solved for the exposure age and inheritance. Finally, we determined ages for depth profiles corrected for inheritance assuming the maximum erosion rates which allow for the accumulation of TCNs and that do not exceed the basin-wide erosion rates determined by the TCN concentrations in stream channel sediments.

4. Results

Using the ^{10}Be TCN concentrations in the stream sediments we have calculated erosion rates that range from 19 to 39 m/Ma with an average of 30.5 ± 6.2 m/Ma (error = 1 S.D.; Fig. 10). The sample (bulk3) in which two different grain sizes were used had erosion rates of 35.4 ± 3.1 and 35.3 ± 2.7 m/Ma. This provides confidence that the grain size used in this analysis reflects the erosion rate. Furthermore, there is no systematic change in erosion rate dependent on catchment

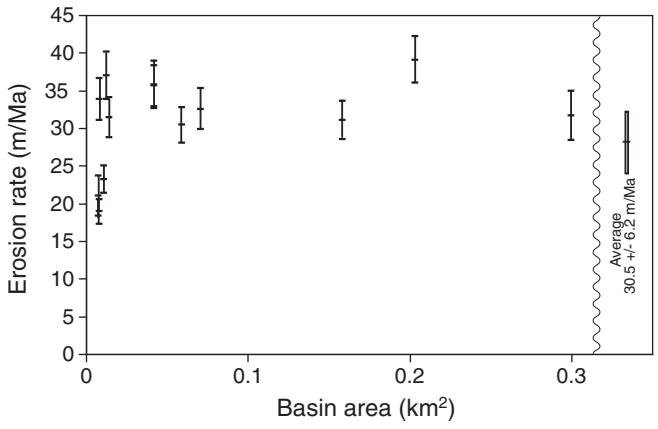

Fig. 10. Beryllium-10 TCN surface exposure ages for boulders plotted by location.

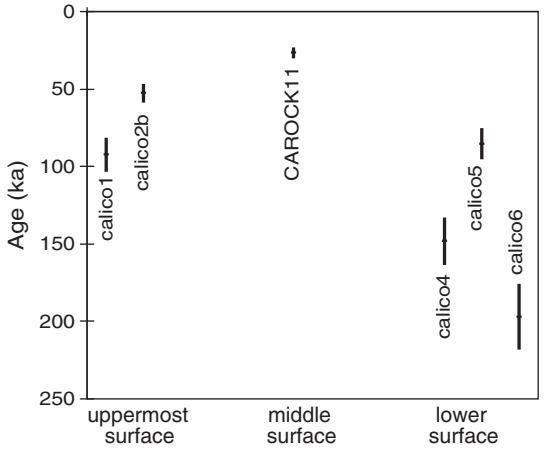

Fig. 11. Erosion rates determined from ^{10}Be TCN concentrations in sediments plotted by size of each catchment area.

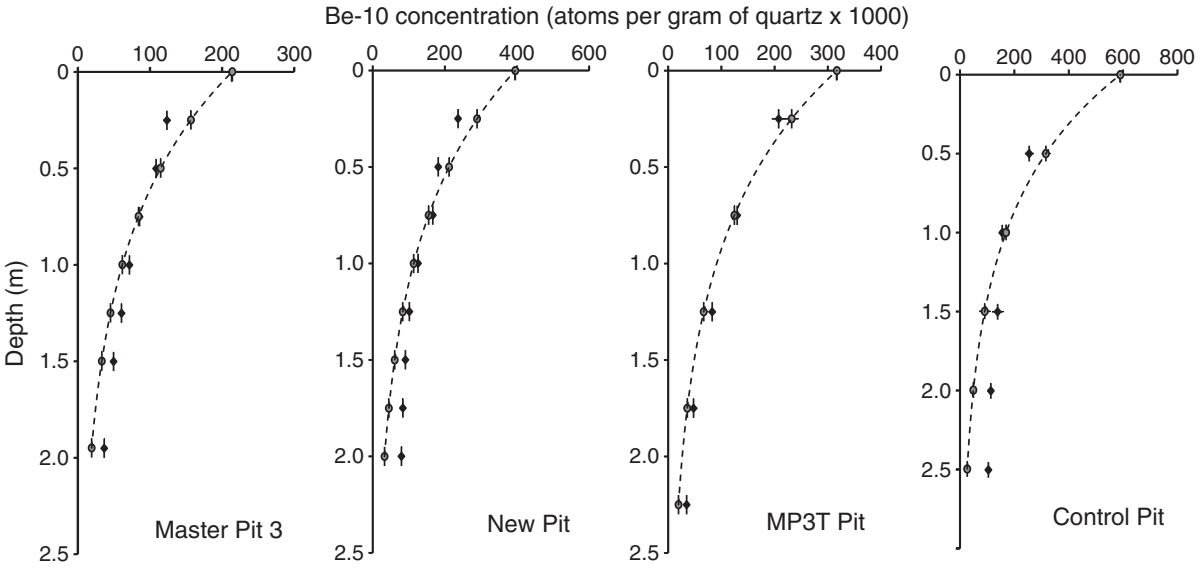

Fig. 12. Depth profile plots for TCNs from the pits examined at the Calico Archaeological Site. The black diamonds are the measured TCN concentrations. The grey circles and the dashed line are modeled TCN concentrations using an attenuation length of 160 g cm^{-2} and a density of 1.9 ± 0.1 g cm^{-3}, and using the surface TCN concentrations calculated from the measured TCN concentrations. The sample measured in the Master Pit at a depth of 175 cm was not included in the analysis because of the extremely large uncertainty.

area size, although the lowest erosion rates are from the smallest catchment areas (Fig. 10). The average includes the lowest values from the smallest catchment area, and therefore the 30.5 ± 6.2 m/Ma value might be an underestimate (Fig. 10).

TCN ages on boulders range from ~27 ka to 197 ka (Table 1). These are plotted in Fig. 11 and show no systematic age relationship between surface height and age. The boulder ages can be used to estimate maximum boulder erosion rates using Eq. (1). The oldest boulder provides the best estimate at 3.3 ± 0.3 m/Ma (Table 1), which is similar to summit boulder erosion rate of Small et al. (1997; 5 m/Ma) for the Sierra Nevada.

Depth profiles for each pit are shown in Fig. 12 and their ages are listed in Table 3. Minimum ages uncorrected for inheritance and erosion range from 31 to 84 ka (Fig. 12). When corrected for maximum allowable erosion the ages range from 43 ka to 139 ka (Fig. 12).

5. Discussion

The ^{10}Be TCN concentrations in stream sediments provide the first quantitative estimates for erosion rates in the Calico Hills. Although very different environments, a basin-wide erosion rate of 30.5 ± 6.2 m/Ma determined from ^{10}Be TCN concentrations in stream sediments is similar to values determined in the Great Smokey Mountains, Bolivian Andes, Tibet Plateau, Dead Sea Rift and Sri Lanka (Matmon et al., 2003; Safran et al., 2005; Chappell et al., 2006; Haviv et al., 2006; Vanacker et al., 2007). This supports the view that our results are consistent with the normal range of erosion in natural settings.

The large range of TCN ages (27–198 ka) for the surface boulders reflects the significant erosion at the site. The oldest boulder (calico6, 198 ± 21 ka) provides a minimum age on the Yermo Deposits, assuming the boulder has no inherited TCNs and the younger TCN ages reflect erosion and exhumation of boulders. Given an erosion rate of 30.5 ± 6.2 m/Ma, then we would expect several meters of surface erosion. This eroded sediment may have significantly shielded the boulders resulting in the younger boulder ages. Alternatively, the oldest age might be interpreted as representing a boulder that had prior exposure to TCN and is an overestimate. This suggests that the surface is likely older than the Late Pleistocene and significant erosion/exhumation has occurred in the study area.

The depth profile ages have similar ages to the boulders. The youngest depth profile age is for Master Pit 3 (~43 ka) located at the lowest position and on the flank of a spur. This surface might have experienced more erosion than the other locations. The other depth profiles are significantly older (83 ka, 135 ka and 139 ka) and suggest an early Late Pleistocene or latest Middle Pleistocene age for the surfaces, and places a minimum age on the Yermo Deposits of latest Middle Pleistocene (~138 ka based on the oldest depth profile).

Debenham (1998, 1999) provided a thermoluminescence age ~135 ka for the Yermo Deposits, but this had extremely large associated errors. Furthermore, Bischoff et al. (1981) used uranium-thorium dating to provide an age of ~200 ka for the deposits and an age of ~100 ka for a relict soil profile within the Yermo Deposits (Bischoff et al., 1981). Our TCN ages support the view that the Yermo Deposits likely formed during the latter part of the Middle Pleistocene or earliest Late Pleistocene.

Our new ages provide a minimum estimate for the ages of the surfaces at the Calico Archaeological Site and hence minimum estimates for the age of the Yermo Deposits. The dating, however, does not resolve the different interpretations of the stratigraphy at the site (Fig. 4). However, irrespective of what interpretation is favored our ages provide a minimum age for the Yermo Deposit and the onset

Table 3
Be-10 TCN depth profile ages. The ages are expressed as minimum estimates for the surfaces.

Depth profile	Production rate (atoms/gram SiO_2)	Age with no inheritance (ka)	Inherited TCNs (atoms/gram SiO_2)	Age corrected for inheritance (ka)	Chi-squared for corrected profile	Age corrected for erosion (ka)
Master Pit 3	6.85	31.2	24650	21.7	8.95	42.8
New Pit	7.00	56.4	53200	35.5	10.2	83.3[a]
MP3T Pit	6.86	46.2	18300	39.2	1.29	134.5[a]
Control Pit	7.00	84.2	89000	39.4	3.46	139.1[a]

[a] Calculated using the upper limit of erosion of 20.5 m/Ma.

of erosion at the Calico Archaeological Site during the latter part of the middle Pleistocene.

A latest Middle Pleistocene or earliest Late Pleistocene age for the Yermo Deposits has significant implications for the archaeology at the Calico Archaeology Site. Our new ages suggest that any artifacts/geofacts found in the Yermo Deposits are of considerable antiquity, and are older than from any other location in North America, which might suggest very early human occupation of North America (c.f. Marshall, 2001).

6. Conclusions

The ^{10}Be TCN concentrations in stream sediments in the Calico Hills show that basin-wide erosion rates range from 19 to 39 m/Ma, with an average of 30.5 ± 6.2 m/Ma. Surface boulders have ^{10}Be TCN ages that range from 27 ka to 198 ka. This wide range of ages probably reflects significant erosion of the Calico Hills. However, the oldest TCN age (198 ± 21 ka) likely places a minimum limit on age of the Yermo Deposits. Depth profile ages at four locations within the study area have minimum ages that range from 31 to 84 ka, but when corrected for erosion the surfaces have ages ranging 43 to 139 ka. These data support the view that the surfaces on the Yermo Deposits likely formed during the Late Pleistocene to latest Middle Pleistocene. This age has important implications for interpreting the context of the artifact/geofacts (Haynes, 1973) that occur within the deposits, which might suggest very early human occupation of North America (c.f. Marshall, 2001). The new ages and erosion rates provide a framework for future paleoenvironmental and landscape evolution studies in this region and in other semi-arid environments.

Acknowledgements

Many thanks to James Bischoff, Andrew Plater and an anonymous reviewer for their very positive and constructive comments on our manuscript; Calico Early Man Site, Inc. for funding this research and their hospitality while we were undertaking our fieldwork and their patience while processing the sample and writing this manuscript; Tim Phillips for drafting Figs. 2 and 4. Thanks to James Bischoff for providing us with the structural data for Fig. 6.

References

Anderson, R.S., Repka, J.L., Dick, G.S., 1996. Dating depositional surfaces using in situ produced cosmogenic radionuclides. Geology 24, 47–51.
Balco, G., Stone, J.O., Lifton, N.A., Dunai, T.J., 2008. A complete and easily accessible means of calculating surface exposure ages or erosion rates from ^{10}Be and ^{26}Al measurements. Quaternary Geochronology 8, 174–195.
Benn, D.I., Owen, L.A., Finkel, R.C., Clemmens, S., 2006. Pleistocene Lake outburst floods and fan formation along the Eastern Sierra Nevada: implications for the interpretation of intermontane lacustrine records. Quaternary Science Reviews 25, 2729–2748.
Bierman, P.R., Steig, E.J., 1996. Estimating rates of denudation using cosmogenic isotope abundances in sediment. Earth Surface Processes and Landforms 21, 125–139.
Bischoff, J.L., Shlemon, R.J., Ku, T.L., Simpson, R.D., Rosenbauer, R.J., Budinger, F.E., 1981. Uranium-series and soils-geomorphic dating of the Calico Archaeological Site, California. Geology 9, 576–582.
Bryan, A.L. (Ed.), 1978. Early man in America from a circum-Pacific perspective: Edmonton, University of Alberta, Department of Anthropology, archaeological Researchers International Occasional Paper, 1 (327 p.).
Budinger Jr., F.E., 2004. Middle- and Late-Pleistocene Archaeology of the Manix Basin, San Bernardino County, California. In: Lepper, B.T., Bonnichsen, R. (Eds.), New Perspectives on the First Americans. Center for the Study of the First Americans, Texas A&M Press, College Station, Texas, pp. 13–25.
Budinger, F.E., Jr., Oberlander, T.M., Thomas, D., 2010. Calico Early Man Site, a World Wide Web Site accessible at URL www.calicodig.org.
Cayan, D.R., Dettinger, M.D., Diaz, H.F., Graham, N.E., 1998. Decadal variability of precipitation over western North America. Journal of Climate 11, 3148–3166.
Cayan, D.R., Redmond, K.T., Riddle, L.G., 1999. ENSO and hydrologic extremes in the western United States. Journal of Climate 12, 2881–2893.
Chappell, J., Zheng, H., Fifield, K., 2006. Yangtse River sediments and erosion rates from source to sink traced with cosmogenic ^{10}Be: Sediments from major rivers. Palaeogeography, Palaeoclimatology, Palaeoecology 241, 79–94.
Cox, B.F., Hillhouse, J.W., Owen, L.A., 2003. Pliocene and Pleistocene evolution of the Mojave River, and associated tectonic development of the Transverse Ranges and Mojave Desert, based on borehole stratigraphy studies and mapping of landforms and sediments near Victorville, California. In: Enzel, Y., Wells, S. and Lancaster, N., (eds.), Paleoenvironment and paleohydrology of the Mojave and southern Great Basin deserts. Geological Society of America Special Paper 368, 1–42.
Debenham, N., 1998. Thermoluminescence Dating of Sediment from the Calico Site (California) (CAL1). Quaternary TL Surveys, Nottingham, United Kingdom.
Debenham, N., 1999. Thermoluminescence Dating of Sediment from the Calico Site (California) (CAL2). Quaternary TL Surveys, Nottingham, United Kingdom.
De Lumley, et al., 1988. Découvert d'outils tailles associés à des faunes du Pléistocène moyen dan a Toca de Esperançe État de Bahia, Brésil. C.R. Academie des Sciences Paris t 306 (II), 241–247.
Dudash, S.L., 2006. Preliminary surficial geologic map of a Calico mountains piedmont and art of Coyote Lake, Mojave Desert, San Bernardino County, California. U.S. Geological Survey Open-File Report 2006-1090.
Enzel, Y., Wells, S.G., Lancaster, N., 2003. Paleoenvironments and Paleohydrology of the Mojave and Southern Great Basin Deserts: Geological Society of America Special Paper 368, Boulder, CO (249 pp.).
Frankel, K.L., Brantley, K.S., Dolan, J.F., Finkel, R.C., Klinger, R.E., Knott, J.R., Machette, M.N., Owen, L.A., Phillips, F.M., Slate, J.L., Wenicke, B.P., 2007a. Cosmogenic ^{10}Be and ^{36}Cl geochronology of offset alluvial fans along the northern Death Valley fault zone: implications for transient strain in the eastern California shear zone. Journal of Geophysical Research, Solid Earth 112, B06407. doi:10.1029/2006JB004350.
Frankel, K.L., Dolan, J.F., Finkel, R.C., Owen, L.A., Hoeft, J.S., 2007b. Spatial variations in slip rate along the Death Valley–Fish Lake Valley fault system determined from LiDAR topographic data and cosmogenic ^{10}Be geochronology. Geophysical Research Letters 34, LI8303. doi:10.1029/2007GL030549.
Gosse, J.C., Phillips, F.M., 2001. Terrestrial in situ cosmogenic nuclides: theory and application. Quaternary Science Reviews 20, 1475–1560.
Hancock, G., Anderson, R., Chadwick, O., Finkel, R., 1999. Dating fluvial terraces with ^{10}Be and ^{26}Al profiles: application to the Wind River, Wyoming. Geomorphology 27, 41–60.
Haviv, I., Enzel, Y., Zilberman, E., Whipple, K., Stone, J., Matmon, A., Fifield, L.K., 2006. Climatic control on erosion rates of dolo-limestone hilltops. Bet-Shean, The Israel Geological Society, Annual Meeting Abstract Book, p. 54.
Haynes, V., 1973. The Calico site: artifacts of geofacts. Science 181, 305–310.
Hereford, R., Webb, R.H., Longpre, C.I., 2007. Precipitation history and ecosystem response to multidecadal precipitation variability in the Mojave Desert region, 1893–2001. Journal of Arid Environments 67, 13–34.
Lal, D., 1991. Cosmic ray labeling of erosion surfaces: in situ nuclide production rates and erosion models. Earth and Planetary Science Letters 104, 429–439.
Le, K., Lee, J., Owen, L.A., Finkel, R.C., 2007. Late Quaternary slip rates along the Sierra Nevada frontal fault zone, California: slip partitioning across the western margin of the Eastern California Shear Zone/Basin and Range Province. Geological Society of America, Bulletin 119, 240–256.
Matmon, A., Bierman, P., Larsen, J., Southworth, S., Pavich, M., Caffee, M., 2003. Erosion of an ancient mountain range, the Great Smoky Mountains, North Carolina and Tennessee. American Journal of Science 303, 817–855.
Matmon, A., Schwartz, D.P., Finkel, R., Clemmens, S., Hanks, T., 2005. Dating offset fans along the Mojave section of the San Andreas fault using cosmogenic ^{26}Al and ^{10}Be. Geological Society of America Bulletin 117, 795–807.
Marshall, E., 2001. PreClovis sites fight for acceptance. Science 291, 1730–1732.
Meek, N., 1989. Physiographic History of the Afton Basin, Revisited. In: Reynolds, R.E. (Ed.), The West-Central Mojave: Quaternary Studies between Kramer and Afton Canyon. San Bernardino County Museum Association, Redlands, California, pp. 78–83.
Meek, N., 1990. Late Quaternary Geochronology and Geomorphology of the Manix Basin, San Bernardino County, California. Unpublished Ph.D. dissertation, University of California, Los Angeles.
Meek, N., 1999. New Discoveries about the Late Wisconsinan History of the Mojave River System. In: Reynolds, R.E., Reynold, J. (Eds.), Tracks Along the Mojave: A Field Guide from Cajon Pass to the Calico Mountains and Coyote Lake. San Bernardino County Museum Association, Redlands, California.
Meighan, C.W., 1983. Early man in the new world. In: Masters, P.M., Flemming, N.C. (Eds.), Quaternary Coastlines and Marine Archaeology: Towards the Prehistory of Land Bridges and Continental Shelves. New York, Academic Press, pp. 441–461.
Meltzer, D.J., 2009. First Peoples in a New World: Colonizing Ice Age America. University of California Press, Berkeley.
Nishiizumi, K., Imamura, M., Caffee, M.W., Southon, J.R., Finkel, R.C., McAninch, J., 2007. Absolute calibration of Be-10 AMS standards. Nuclear Instruments and Methods in Physics Research. Section B: Beam Interactions with Materials and Atoms 258, 403–413.
Owen, L.A., Finkel, R.C., Caffee, M.W., Gualtieri, L., 2002. Timing of multiple glaciations during the Late Quaternary in the Hunza Valley, Karakoram Mountains, Northern Pakistan: defined by cosmogenic radionuclide dating of moraines. Geological Society of America Bulletin 114, 593–604.
Rogers, T.H., 1967. Geological map of California: San Bernardino sheet. California Division of Mines and Geology; scale 1:250, 000.
Safran, E.B., Bierman, P.R., Aalto, R., Dunne, T., Whipple, K.X., Caffee, M., 2005. Erosion rates driven by channel network incision in the Bolivian Andes. Earth Surface Processes and Landforms 30, 1007–1024.
Shlemon, R.J., Budinger Jr., F.E., 1990. The archeological geology of the Calico site, Mojave Desert, California. Geological Society of America, Centennial Special, vol., 4, pp. 301–313.
Small, E.E., Anderson, R.S., Repka, J.L., Finkel, R.C., 1997. Erosion rates of alpine bedrock summit surfaces deduced from in-situ Be-10 and Al-26. Earth and Planetary Science Letters 150, 413–425.

Stone, J.O., 2000. Air pressure and cosmogenic isotope production. Journal of Geophysical Research 105, 23,753–23,759.

Taylor, R.E., Payen, L.A., 1979. The role of archaeometry in American archaeology: approaches to the evaluation of the antiquity of Homo sapiens in California. In: Schiffer, M.B. (Ed.), Advances n archaeological method and theory 2. New York, Academic Press, pp. 239–283.

Van Devender, T.R., 1990. Late Quaternary vegetation and climate of the Sonoran Desert, United States and Mexico. In: Betancourt, J.L., et al. (Ed.), Packrat middens: the last 40,000 years of biotic change. University of Arizona Press, Tucson, pp. 134–165.

Vanacker, V., von Blanckenburg, F., Hewawasam, T., Kubik, P.W., 2007. Constraining landscape development of the Sri Lankan escarpment with cosmogenic nuclides in river sediment. Earth and Planetary Science Letters 253, 402–414.

Zehfuss, P.H., Bierman, P.R., Gillespie, A.R., Burke, R.M., Caffee, M.W., 2001. Slip rates on the Fish Springs fault, Owens Valley, California, deduced from cosmogenic ^{10}Be and ^{26}Al and soil development on fan surfaces. Geological Society of America Bulletin 113, 241–255.